ACS OMEGA

Open Access

http://pubs.acs.org/journal/acsodf

Article

Biosorption Potential of *Arachis hypogaea*-Derived Biochar for Cd and Ni, as Evidenced through Kinetic, Isothermal, and Thermodynamics Modeling

Fozia Batool,* Rahman Qadir, Fatima Adeeb, Samia Kanwal, Ehab A. Abdelrahman, Sobia Noreen, Bedur Faleh A. Albalawi, Muhammad Mustaqeem, Muhammad Imtiaz, Allah Ditta,* and Humaira Yasmeen Gondal

Cite This: *ACS Omega* 2023, 8, 40128−40139

Read Online

ACCESS | Metrics & More | Article Recommendations | Supporting Information

ABSTRACT: Biochar derived from plant biomass has great potential for the decontamination of aqueous media. It is the need of the hour to test biochar derived from economical, easily available, and novel materials. In this regard, the present study provides insight into the sorption of two heavy metals, i.e., cadmium (Cd) and nickel (Ni), using native *Arachis hypogaea* and its biochar prepared through pyrolysis. The effect of different factors, including interaction time, initial concentration of adsorbate, and temperature, as well as sorbent dosage, was studied on the sorption of Cd and Ni through a batch experiment. Characterization of the native biowaste and prepared biochar for its surface morphology and functional group identification was executed using Fourier transform infrared (FTIR) spectroscopy and scanning electron microscopy (SEM). Results revealed the presence of different functional groups such as −OH on the surface of the adsorbent, which plays an important role in metal attachment. SEM reveals the irregular surface morphology of the adsorbent, which makes it easy for metal attachment. Thermogravimetric analysis shows the stability of *A. hypogaea* biochar up to 380 °C as compared with native adsorbent. The adsorption efficacy of *A. hypogaea* was found to be higher than that of native *A. hypogaea* for both metals. The best adsorption of Cd (94.5%) on biochar was observed at a concentration of 40 ppm, an adsorbent dosage of 2 g, a contact time of 100 min, and a temperature of 50 °C. While the optimum conditions for adsorption of Ni on biochar (97.2% adsorption) were reported at a contact time of 100 min, adsorbent dosage of 2.5 g, initial concentration of 60 ppm, and temperature of 50 °C. Results revealed that biochar offers better adsorption of metal ions as compared with raw samples at low concentrations. Isothermal studies show the adsorption mechanism as physical adsorption, and the negative value of Gibb's free energy confirms the spontaneous nature of the adsorption reaction. An increase in entropy value favors the adsorption process. Results revealed that the sorbent was a decent alternative to eliminate metal ions from the solution instead of costly adsorbents.

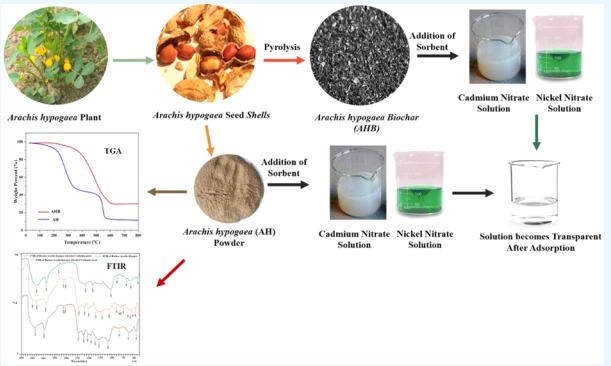

INTRODUCTION

Since the beginning of the modern era, environmental pollution is posing adverse effects on the globe and has now turned into a major ecological problem.[1,2] Several factors including global warming, depletion of the ozone layer, desertification, discharge of industrial effluents, and toxic compounds have increased the intensity of this issue.[3] We are living in an era where tons of waste, especially industrial effluents, are produced every day and get dissolved in the drinking water and groundwater.[4] These wastes carry heavy metals (HMs) that might be dangerous even in small quantities. Our soil, air, and water mediums are severely contaminated by HMs like magnesium (Mg), nickel (Ni), mercury (Hg), cadmium (Cd), chromium (Cr), lead (Pb), and arsenic (As) and therefore there is a dire need to protect the aquatic environment from such HMs due to their non-biodegradable and toxic nature.[5,6] HMs are persistently present in our environment, as they cannot be degraded by biological or any other organism.[7] Their presence in water in an ionic form can affect aquatic life and sometimes endanger aquatic life.[8]

HMs, such as Cd and Ni, although present in low concentrations, adversely affect human beings and cause respiratory problems, immunological weakness, kidney and liver disorders, hypertension, genetic and neurological changes,

Received: May 1, 2023
Accepted: October 2, 2023
Published: October 18, 2023

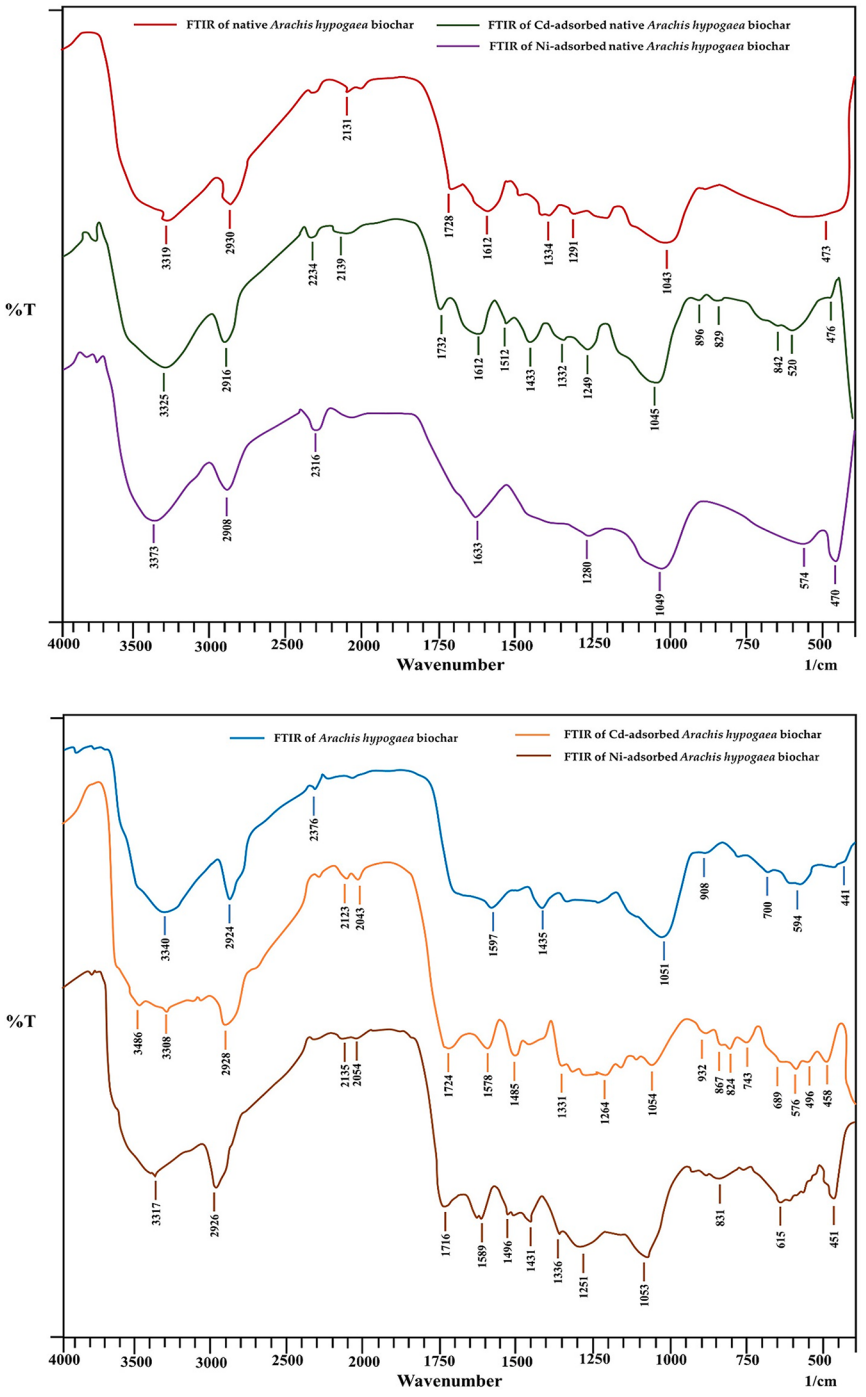

Figure 1. FTIR spectra of native *A. hypogaea* and *A. hypogaea* biochar before and after adsorptionA clear shift in the band position of − OH is observed before and after the adsorption of metal ions from 3319 to 3325 and 3373 cm^{-1} for Ni and Cd ions attachment on native *A. hypogaea*, respectively. Similarly, for biochar, the −OH peak was obtained at 3340 cm^{-1}, which shifted to 3486 and 3317 after Ni and Cd attachment with the surface of the adsorbent. A similar trend is reported by other researchers.[33,34]

cancer, and even lead to death.[9−11] HMs have a toxic nature that links to protein-containing compounds and thus affects their efficiency as well as their structures.[12,13] Several methodologies, such as precipitation, sorption, electrochemical techniques, filtration, sublimation, and floatation, have been employed and amended to eliminate the toxic HMs from wastewater.[12,14−16] Among these methods, adsorption is the most economical and easy approach for the removal of unwanted metals from wastewater.[17,18]

One of the most critical points in the use of adsorbents is the suitability of their porous structures, adsorption velocity, and total adsorption capacity. A wide variety of solid materials can be used as organic carbon and adsorbents, but biochar (BC) is the most economical and cost-effective carbonaceous product.[19−21] Major biomass materials used to prepare biochar are peanut shells, ryes, grass, rice husks, garlic stalk, straw, metropolitan solid waste, and wood waste products. An increase in the carbon content improves the biochar resistance to microbial decomposition. Presently, researchers are trying to investigate its usage

https://doi.org/10.1021/acsomega.3c02986
ACS Omega 2023, 8, 40128−40139

as a soil conditioner.[22] Favorable as well as encouraging use of this material in waste administration has been found. Nowadays, groundwater is continuously being deteriorated due to HMs and other pollutants. Recent studies have shown that biochar can adsorb harmful metals such as Cd, Hg, Cr, Pb, Zn, Cu, and Ni from wastewater.[23,24]

However, it is pertinent to observe the behavior of sorbent by correlating the sorbent equilibrium with selected parameters under specified conditions.[25] Such correlations can be studied by employing the equilibrium isotherms that in turn sort out the monolayer/multilayer sorption processes based on the interaction between the sorbent and its surface.[26−28] Similarly, the spontaneity of the adsorption process can be explained based on thermodynamic studies. Other factors, such as suitable temperature range and the nature of both sorbent and sorbate at equilibrium, can also be explained using these studies.[29,30]

In the present study, the adsorptive removal of Cd and Ni from the aqueous medium was tested using the raw biomass of *Arachis hypogaea* peels and its biochar. To our knowledge, no study has been conducted that involved the use of the raw biomass of *Arachis hypogaea* peels and its biochar as adsorbents. The synthesis of biochar was carried out from locally available waste biomass, i.e., peels of *Arachis hypogaea* (commonly known as peanut). The waste biomass could be easily obtained from house dustbins and from factories that use peanuts in their products such as biscuits and bakeries. The prepared biochar was further employed in the adsorption of Cd and Ni from the aquatic medium under selected parameters such as pH, initial concentration of sorbate, contact time, and concentration of sorbent. Moreover, isothermal, kinetic, and thermodynamic studies were conducted to observe the nature of the reaction.

RESULTS AND DISCUSSION

The adsorption potential of biochar synthesized from synthetic *A. hypogaea* and native *A. hypogaea* was used to eliminate Cd and Ni from the aqueous solution.

Characterization of Sorbent. Characterization of the sorbent is a crucial factor of measurement. Surface morphology and functional groups present in the sorbent can be characterized by employing scanning electron microscopy and Fourier transform infrared spectroscopy, respectively.

Fourier Transform Infrared (FTIR) Spectroscopy. Results obtained from FTIR analysis of AH and AHB before and after the adsorption of Cd and Ni are listed in Figure 1. The hydroxyl group peak appears in the range of 3501−3009 cm^{-1}, while the hydroxyl group (O−H) adsorption band appears at 3346 cm^{-1} and also on 3319.49 cm^{-1} before the sorption for biochar as well as native *A. hypogaea*. Inter- and intramolecular hydrogen bonding is accountable for stretching along with the broadening of the band of −OH in the FTIR spectrum. For the C−H bond, the range was 2920−2900 cm^{-1}. A peak observed at 2341.58 cm^{-1} might be linked with C═N. Peaks in the range of 2001−1550 cm^{-1} are due to the C═C stretching vibrations in both adsorbents. For adsorption purposes, a significant role is played by the −OH group and heteroatoms to attach sorbate on the surface.[31,32]

Scanning Electron Microscopy (SEM). The surface morphology of *A. hypogaea* is determined by scanning electron microscopy. Images of SEM of biochar and native *A. hypogaea* are shown in Figure 2. It is indicated from the images that the surface of the sorbent is rough and irregular, which enhances the speed of HM adsorption on the sorbent surface.[33,35]

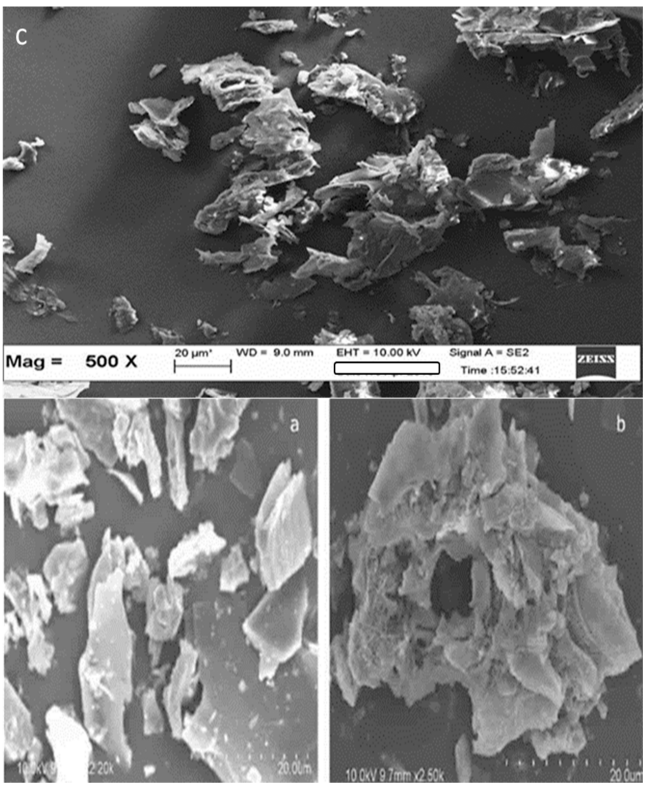

Figure 2. SEM image of *A. hypogaea* (a, b) Native *A. hypogaea*, (c) *A. hypogaea* Biochar.

Thermogravimetric Analysis. Thermogravimetric analysis was performed to analyze the thermal stability of native *A. hypogaea* and its biochar. Results given in Figure S1 show that a loss of 5.5% of the weight was observed for native *A. hypogaea* from room temperature up to 150 °C due to moisture content present in the native adsorbent. This kind of weight loss is not observed for biochar samples, as it is already treated at high temperatures and contains no moisture content. A significant weight change was observed from 250 to 320 °C due to the decomposition of major constituents of native *A. hypogaea*. These components are cellulose, hemicellulose, and lignin, which contribute a major part in the mass of *A. hypogaea*. Cellulose starts decomposing at 275 °C and hemicellulose above 150 °C, while lignin shows degradation at 250 to 500 °C.[36,37] So change in weight represented by arrow 1 may be due to cellulose and hemicellulose, while arrow 2 shows weight loss due to lignin decomposition. In *A. hypogaea* biochar a major weight change was observed at 350 °C due to lignin loss. Research outputs are in good agreement with the reported data.[38]

Absorption Study and Optimization of Parameters. The absorption study was based on the batch absorption method, and the surface parameters such as initial concentration of sorbate, interaction time, and concentration of sorbent were optimized to verify the best adsorption conditions for the sorbent (Figures S2 and S3). The stirring speed of the orbital shaker was kept at 150 rpm to observe the adsorption of Cd and Ni on raw and biochar *A. hypogaea*.

Effect of pH. Adsorption of metal ions is highly dependent on the pH factor as surface charge and metal ion attachment on the surface are decided by this factor. To optimize the factor of pH for the removal of Cd and Ni ions on AH and AHB, the experiment was performed in the pH range 1−7, as shown in Figure S2. As metal ions start precipitation in the basic pH range,

https://doi.org/10.1021/acsomega.3c02986
ACS Omega 2023, 8, 40128−40139

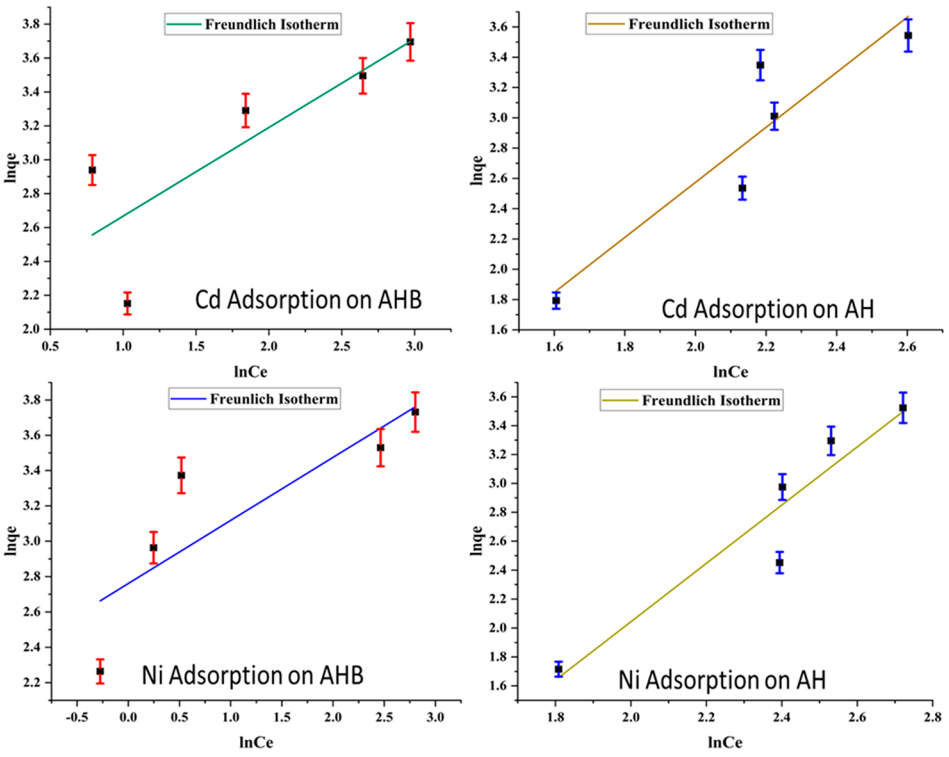

Figure 3. Freundlich isotherm for the adsorption of Cd and Ni on *A. hypogaea* (AH) and *A. hypogaea* biochar (AHB).

the adsorption experiment was not extended above pH range 7. Adsorption efficiency was found to be small at low pH, as the oxygen of the adsorbent surface is protonated by an acidic pH range. However, a positive trend in the adsorption rate was observed by increasing the pH of the adsorption solution, and maximum adsorption potential was achieved at pH 6 for both metal ions. The optimization of other parameters (concentration of sorbate, contact time, amount of adsorbent, and temperature) discussed below was conducted at pH 6.

Concentration of Sorbate. To estimate the effect of changes in the concentration of HMs, solutions of varying concentrations such as 20, 40, 60, 80, and 100 ppm were prepared by adding 1 g of sorbent and stirring at a speed of 150 rpm for biochar and native *A. hypogaea*. These solutions were placed in an orbital shaker for 90 min and filtered. Atomic absorption spectroscopy was further employed to analyze the adsorption of Cd and Ni.

It was observed that the amount of Ni adsorption was found gradually increased with an increase in Ni ion concentration, and the maximum amount of Ni was adsorbed at 80 ppm initial concentration for both biochar and native *A. hypogaea*. By increasing Ni ion concentration more ions are available to attach on the surface of the adsorbent, so a positive trend in adsorption was observed but further raise in concentration have no prominent effect on the rate of adsorption as the surface of the adsorbent is completely saturated by metal ions and no more spaces are available to attach metal ions.[36,39] The removal of the Cd ion concentration increased because of the positive effect of both biochar and native *A. hypogaea*; however, adsorption on biochar was found higher for both metal ions. Biochar provides an increase in surface area and hence more active sites for the attachment of these metal ions (Figure S3). These findings are in line with Tong et al.[40] and Tungala et al.[41]

Contact Time. Contact time has been found to increase the ratio of metal adsorption for both metal ions on biochar and native *A. hypogaea*. Contact time was varied from 20 to 100 min and metal attachment enhanced as contact time was increased. Adsorption was found to reach 94% at 100 min of contact time for Ni on biochar and 81% on native *A. hypogaea*. Similarly, the Cd adsorption rate was found to be promising (93.5%) for biochar and 82% for native *A. hypogaea*. Initially, a sharp increase in adsorption rate was observed when contact time was increased from 20 to 40 min, but then adsorption increased slowly as active sites are gradually occupied by metal ions and less number of spaces are available. A similar trend is observed for the adsorption of other metal ions in reported data.[42]

Amount of Adsorbent. The amount of adsorbent is also considered to have a promising effect on the adsorption of metal ions. The amount of adsorbent was varied from 0.5 to 2.5 g and the adsorption experiment was repeated with 150 rpm shaking speed and 80 min contact time. Initially, a sharp increase in adsorption rate was observed for all the metal ions, as the amount of adsorbent provides attachment points to these metal ions and adsorption potential was found significant.

Temperature. The adsorption process is greatly affected by the temperature of the adsorption media, as an increase in temperature mostly causes an upshift in the adsorption rate due to an increase in the random movement of the metal ions. A similar trend was shown by Cd and Ni in the present study, as the temperature was raised, adsorption was found to increase up to 40 °C. However, further increases in temperature to 50 °C have found no significant addition to the adsorption rate; even for Cd on native *A. hypogaea*, a decrease in adsorption was observed. Due to an increase in temperature, the entropy of the system increased and this random movement of agro-waste particles enhanced their adsorption efficiency. The results are in line with Wu et al.[30]

Isothermal Study. Adsorption isotherms are generally proposed to properly correlate the interaction between the sorbate concentration and its accumulation on the surface of the

https://doi.org/10.1021/acsomega.3c02986
ACS Omega 2023, 8, 40128−40139

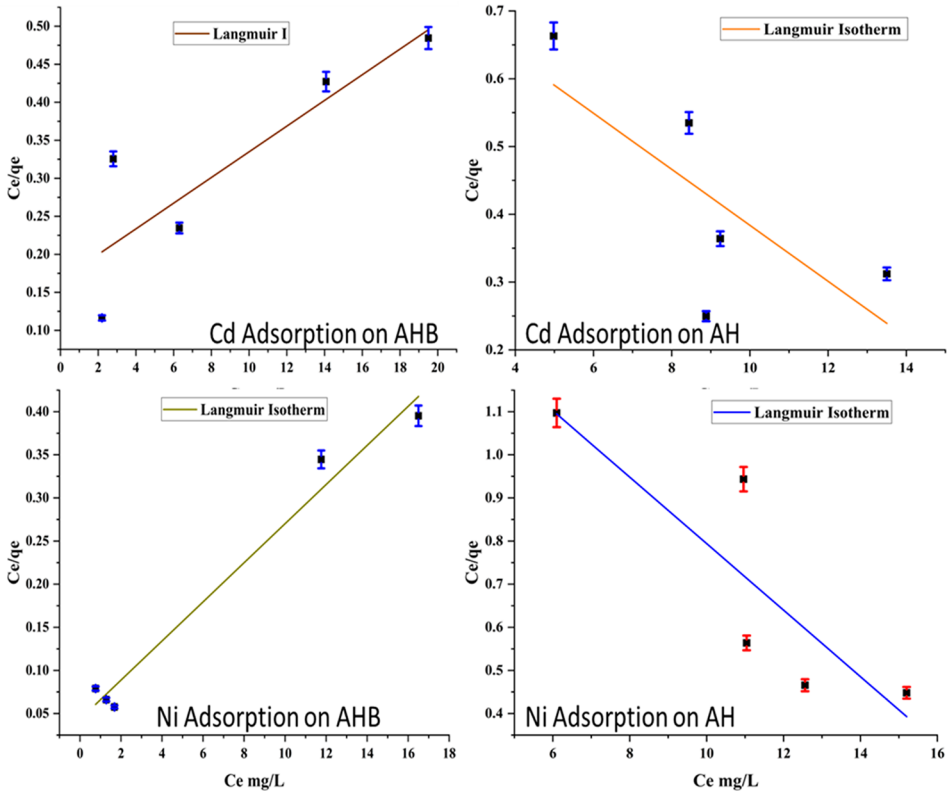

Figure 4. Langmuir adsorption isotherm of Cd and Ni on raw *A. hypogaea* (AH) and *A. hypogaea* biochar (AHB).

Table 1. Linear Parameters of Isothermal Models for the Sorption of Cd and Ni

	adsorption parameters for Cd removal		adsorption parameters for Ni removal	
models	raw *A. hypogaea*	*A. hypogaea* biochar	raw *A. hypogaea*	*A. hypogaea* biochar
Freundlich				
K_F (mg/g)	0.35	8.53	0.14	15.80
n	0.55	1.92	0.50	2.86
R^2	0.85	0.68	0.90	0.72
Langmuir				
Q_o (mg/g)	1.26	6.02	0.64	23.26
K_L/b	−30.42	356.67	−8.31	1057.08
R_L	−0.00033	2.80×10^{-05}	−0.0012	9.46×10^{-06}
R^2	0.54	0.93	0.73	0.96
Dubinin−Radushkevich				
k_{ad} (mol^2/kJ^2)	9.59×10^{-06}	1.15×10^{-06}	1.40×10^{-05}	3.22×10^{-07}
q_s (mg/g)	40.45	32.69	37.34	39.25
R^2	0.84	0.52	0.82	0.96
Temkin				
B (J/mol)	36	11.70	29	8.30
K_T	0.24	1.37	0.17	7.94
R^2	0.79	0.84	0.79	0.84
Elovich				
Q_m (mg/g)	−31.75	−1.79	−28.74	20
K_E	0.22	0.22	−0.26	0.22
R^2	0.74	0.83	0.92	0.41

sorbent at a maintained temperature. In this regard, a particular design may be optimized to remove the effluents from the aqueous system and different adsorption systems such as Langmuir, Freundlich, Redlich−Peterson, Temkin, and Elovich can also be utilized.[37,42,43]

Freundlich Isotherm of Adsorption. Freundlich adsorption isotherm is based on the concept of multilayer adsorption on sorbent and is developed for the heterogeneous system. This is completely explained by the linearized formula.

$$\ln q_e = 1/n \ln C_e + \log C_m$$

where C_{ads} (mol g^{-1}) and C_e (mol g^{-1}) be there for equilibrium concentrations of sorbate, whereas C_m (mmol g^{-1}) depicts the multilayer adsorption and $1/n$ stands for the constant degree of

https://doi.org/10.1021/acsomega.3c02986
ACS Omega 2023, 8, 40128−40139

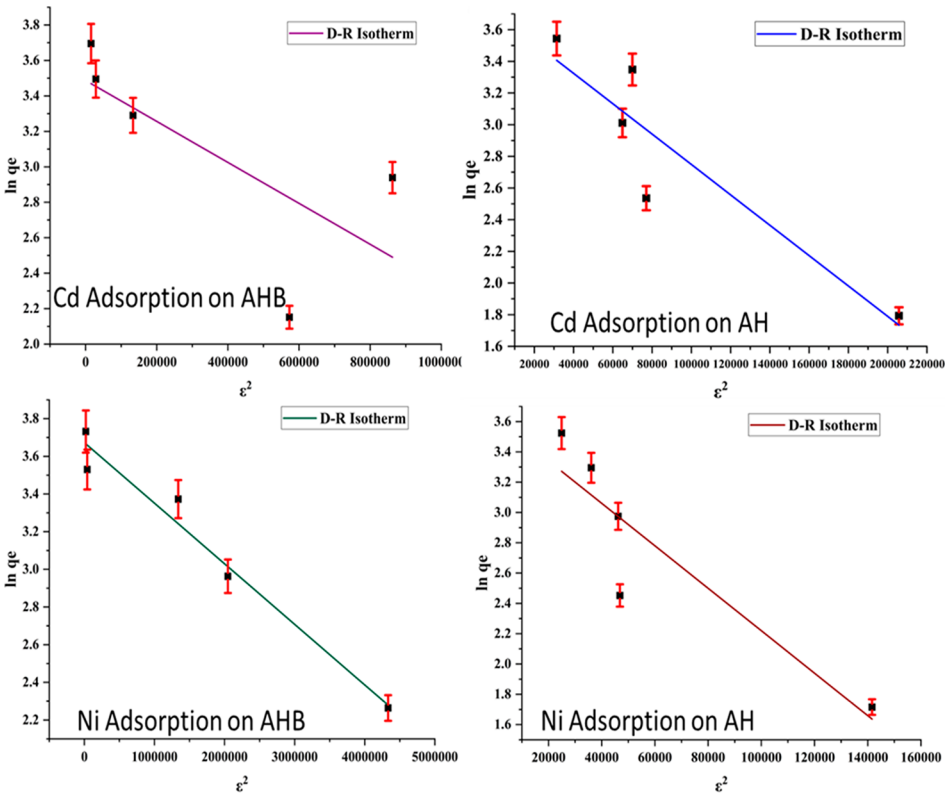

Figure 5. Dubinin−Radushkevich isotherm for adsorption of Cd and Ni on raw *A. hypogaea* (AH) and *A. hypogaea* biochar (AHB).

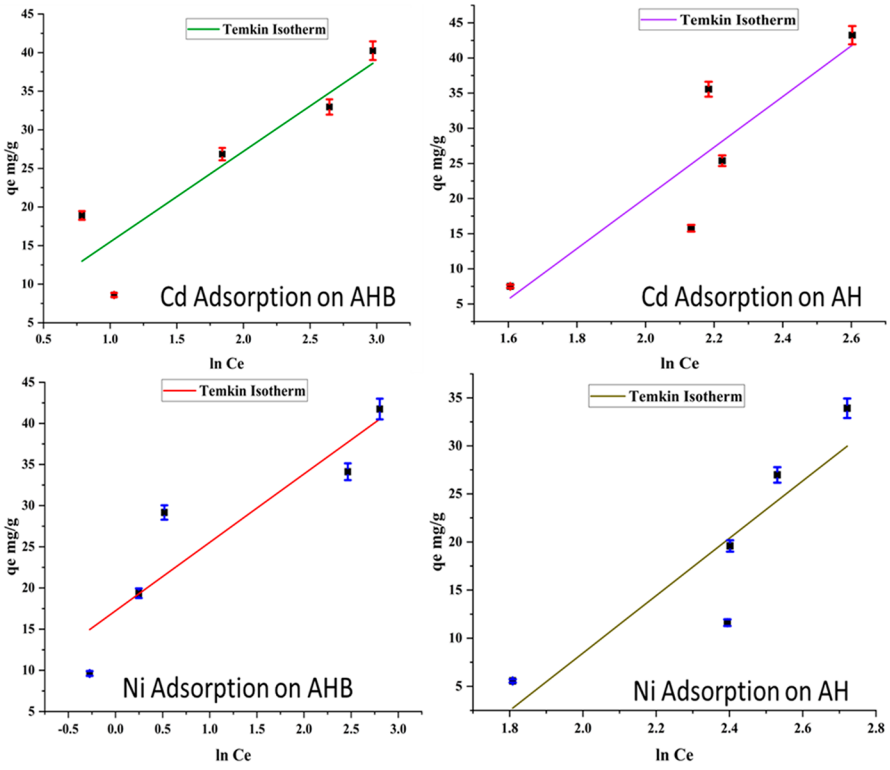

Figure 6. Temkin adsorption isotherm for Cd and Ni on raw *A. hypogaea* (AH) and *A. hypogaea* biochar (AHB).

concentration of adsorption.[38,44] Figure 3 presents the Freundlich isotherm for the adsorption of Ni and Cd on biochar *A. hypogaea* and native *A. hypogaea*, respectively.

Freundlich adsorption capacity (*KF*) indicates the feasibility of the system, if its value is ranging from 1 to 20, then the adsorption process is considered favorable, and here in the current work, *KF* was 8.5 and 15.7, for Cd and Ni adsorption on *A. hypogaea* Biochar, respectively. Similarly, other parameters such as adsorption intensity (*n*) at 1.9 and 2.85 and the values of R^2 (0.685 and 0.72) for Cd and Ni, respectively, were found to

https://doi.org/10.1021/acsomega.3c02986
ACS Omega 2023, 8, 40128−40139

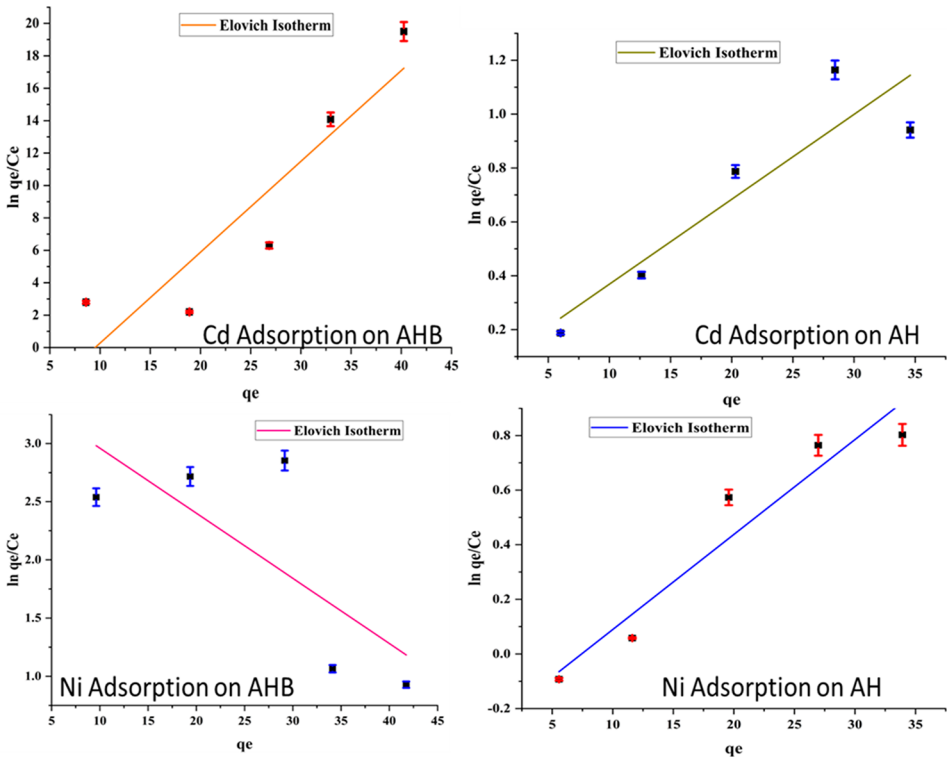

Figure 7. Elovich isotherm for adsorption of Cd and Ni on raw *A. hypogaea* (AH) and *A. hypogaea* biochar (AHB).

be significant and might be linked to the fitness of the model applied.

Langmuir Adsorption Isotherm. In this model, the relationship of adsorption concentration is studied and is usually applied to monolayer adsorbents that have homogeneous and smooth surfaces. Each site is held by one molecule at a constant energy level of the adsorption system. However, practically it is not possible hence all particles have equal surfaces and there is no interaction of adsorbate with molecules.[45,46]

Adsorption of sorbate on saturated sorbent at specific homogeneous places is considered by the Langmuir isotherm. To calculate the Langmuir model, the distribution of metal ions between liquid and solid surfaces was calculated by the equation given below, which shows the relationship of linearity.

$$C_e/q_e = C_e/Q + 1/Q_b$$

Here, Q stands for the adsorption capacity of the sorbent and b (L mol^{-1}) for perpetual energy for sorption. This process is not temperature-dependent. Figure 4 shows the Langmuir isotherm for the adsorption of Ni and Cd on biochar and native biomass.

The initial concentration of RL (a dimensionless value) offers the applicability of the model for a system and if it ranges between 0 and 1, the system is more suitable for the adsorption and the results given in Table 1 lie within this range. Furthermore, the value of R^2 was also near 1, which authenticates the validity of the model used for the present work.

Dubinin−Radushkevich Isotherm. Dubinin−Radushkevich isotherm is based on the empirical model that is much more generalized than Langmuir due to the exclusion of a homogeneous surface and constant sorption potential (Figure 5).

This isotherm generally deals with the adsorption of vapors on heterogeneous systems (solid/liquid), and the results are presented in Table 1. Here the slope of the plot gives the value k_{ad}, and the intercept is q_s. The model offered good feasibility of the adsorption system with a high value of R^2 (0.959) near 1. This isotherm has found very promising applications in determining the nature (physical and chemical) of adsorption. The relationship used to determine the Dubinin isotherm was

$$\ln(q_e) = \ln(q_s) - k_{ad}\varepsilon^2$$

Temkin Isotherm. As the contact between the sorbent and sorbate weakens, the value of the model or isotherm also decreases by keeping the heat of the adsorption variable (Figure 6). To determine Temkin isotherm, the following relationship is used.

$$Q_e = (RT/\Delta Q)\ln K_T + (RT/\Delta Q)\ln C_e$$

In this equation, "R" is the universal gas constant (8.314 J mol^{-1} K^{-1}), T is the temperature (30 °C or 303 K), and ΔQ gives the value of heat transferred in J mol^{-1}, while K_T is constant in the Tempkin model.

The information on binding energy is given by the equilibrium constant of binding K_T, as given in Table 1. The model expresses the exothermic nature of the adsorption reaction as the value of B is greater than zero because heat is released in the process.[37,47,48]

Elovich Isotherm. As per Elovich's model, the mechanism of adsorption was based on the chemical reactions, which are responsible for adsorption (Figure 7). The following relationship was used for the Elovich isotherm model:

$$\ln q_e/C_e = \ln K_E Q_m - q_e/Q_m$$

The plot of $\ln q_e/C_e$ versus q_e gives an R^2 value that is close to unity, whereas the value of K_E (intercept) and Q_m (slope of the plot) represent the initial adsorption rate and adsorption

https://doi.org/10.1021/acsomega.3c02986
ACS Omega 2023, 8, 40128−40139

constant, respectively. Furthermore, the value of R^2 was also close to unity, which authenticates the applicability of the model.

Thermodynamic Studies. Literature shows that temperature has a promising effect on the adsorption capacity of the adsorbent.[38] Adsorption of both metal ions was measured at variable temperature ranges by employing native *A. hypogaea* and *A. hypogaea* biochar as given in Table 2. Temperature was found to have a positive impact on the adsorption rate; as the temperature increases, diffusion of particles becomes high and adsorption is increased.

Table 2. Thermodynamic Parameters for Adsorption of Cd and Ni

	thermodynamic parameters measured based on experimental results				
metals adsorbed	temp (K)	ΔG° (kJ mol^{-1})	ΔH° (kJ mol^{-1})	ΔS° (J mol^{-1} K^{-1})	R^2
Cd adsorption on raw AH	293	−3.099	36.074	111.91	0.92
	303	−2.621			
	313	−0.751			
	323	−0.023			
Cd adsorption on AH biochar	293	−3.307	25.614	92.12	0.94
	303	−3.817			
	313	−5.134			
	323	−6.161			
Ni adsorption on raw AH	293	−2.217	8.073	20.20	0.90
	303	−1.877			
	313	−1.657			
	323	−1.629			
Ni adsorption on AH biochar	293	−1.932	38.211	124.71	0.92
	303	−0.375			
	313	−1.262			
	323	−1.668			

A plot of ln Kl vs $1/T$ was obtained for metal ions adsorption on both adsorbents, as given in Figure 8. The value of enthalpy (ΔH_o) and entropy (ΔS_o) was obtained from slope and intercept, respectively. Gibb's free energy was calculated by employing the equation.

A negative value of Gibb's free energy reflects the spontaneous nature of the adsorption process and positive results for Entropy and Enthalpy show the endothermic nature of the reaction as well as an increase in randomness during the adsorption process.[45]

Kinetic Studies. The time required for the adsorption process to attain equilibrium is determined by kinetic studies. For this purpose, pseudo first order (PFO) and pseudo second order (PSO) kinetic models were applied to the results to determine the mechanism of adsorption (Figure 9). For PFO kinetics, contact time was plotted against $\ln(q_e - q_t)$, and for PSO kinetics contact time was plotted against t/q_t.

Results show that adsorption of Cd on native *A. hypogaea* follows PSO kinetics with a R^2 value of 0.91, and for *A. hypogaea* biochar, better results were obtained with the PFO model, giving a R^2 value of 0.929 (Figure 10). Similarly, for the adsorption of Ni on native and *A. hypogaea* biochar, PSO order kinetics fit better with R^2 0.9 and 0.97, respectively. According to the PFO kinetic model, physisorption is the rate-limiting step in the adsorption mechanism, and the PSO model describes the adsorption capacity of the system. The results are in line with Kochar et al.[49] and Ke et al.[50]

Adsorbent Reuse/Regeneration. Adsorbents used in the present work can be regenerated and reused for the removal of pollutants with a satisfactory removal percentage, as shown in Figure 11. *A. hypogaea* (AH) and *A. hypogaea* biochar (AHB) were regenerated by treating with 0.1 M HCl for 1 h. The adsorbent was thoroughly washed with HCl to remove adsorbed metal ions from the surface and again utilized for metal uptake. Adsorbents were found to be stable, and regenerated adsorbents perform satisfactory uptake of metal ions. Regeneration adds value to the adsorption mechanism in terms of reduction in cost and waste management.

CONCLUSIONS

The present work utilized a seed waste material for the decontamination of Cd and Ni from wastewater. A comparison of the metal removal efficiency of native *A. hypogaea* and its biochar was made to remove Cd and Ni from the aqueous media. The adsorption efficiency of native *A. hypogaea* was 82.5 and 84.8%, while that of *A. hypogaea* biochar was 94.5 and 97.2% for Cd and Ni, respectively. Isothermal and kinetic studies reveal that the adsorption system follows multilayer adsorption with a physisorption mechanism. Thermodynamic studies revealed the spontaneous nature of adsorption with an increase in the system entropy. This study adds a significant contribution in terms of plant waste material reuse for environmental decontamination.

MATERIALS AND METHODS

Preparation of Biochar from *A. hypogaea* L. *Arachis hypogaea* (AH) seed cover was washed with deionized water to remove any surface impurities. After proper drying of AH, it was crushed into a powder, and then the powder was changed into biochar by the process of pyrolysis. For pyrolysis, it was kept in a furnace under an anaerobic environment at 450 °C for 1.5−2 h. This treatment changes it into a dark brown color biochar called *A. hypogaea* biochar (AHB), which is harmless and easy to use for sorption. Dried AH and AHB were ground and passed through a 100-mesh sieve to obtain uniform particle sizes (2 mm) of adsorbents. Fine particle size offers more surface area for adsorption. Prepared adsorbents were stored in airtight bags for further use. Two HMs, i.e., Ni and Cd were selected as sorbents to evaluate the adsorption potential of native *A. hypogaea* and *A. hypogaea* biochar.

Characteristics of Biochar Adsorbent. Functional group and surface analysis methods were applied to determine the characteristics of biochar. Functional group analysis was performed by Fourier transform infrared spectroscopy (FTIR; Model No: Shimadzu FTIR 8400S, Kyoto, Japan) by employing a diffused reflectance infrared technique (DRIFT). In this technique, the adsorbent was mixed with potassium bromide (KBr) to obtain a FTIR spectra. The surface morphology was analyzed by SEM (FEI Nova, Nano-SEM 450, Lausanne, Switzerland). In brief, the electron beam was skimmed through a raster-scan design, and the image was made through the positioning of the beam, which responded with a concentration of the recognized signal. The resolution of the SEM was approximately 1 nm. The thermal stability of native *A. hypogaea* and *A. hypogaea* biochar was determined to evaluate the effective use of adsorbent under different temperature conditions by employing a thermal analyzer (Model No: Mettler Toledo Star SW 9.01, Greifensee, Switzerland).

Adsorption Experiment. Sorption was performed by batch adsorption methods to estimate the effect of different factors

https://doi.org/10.1021/acsomega.3c02986
ACS Omega 2023, 8, 40128−40139

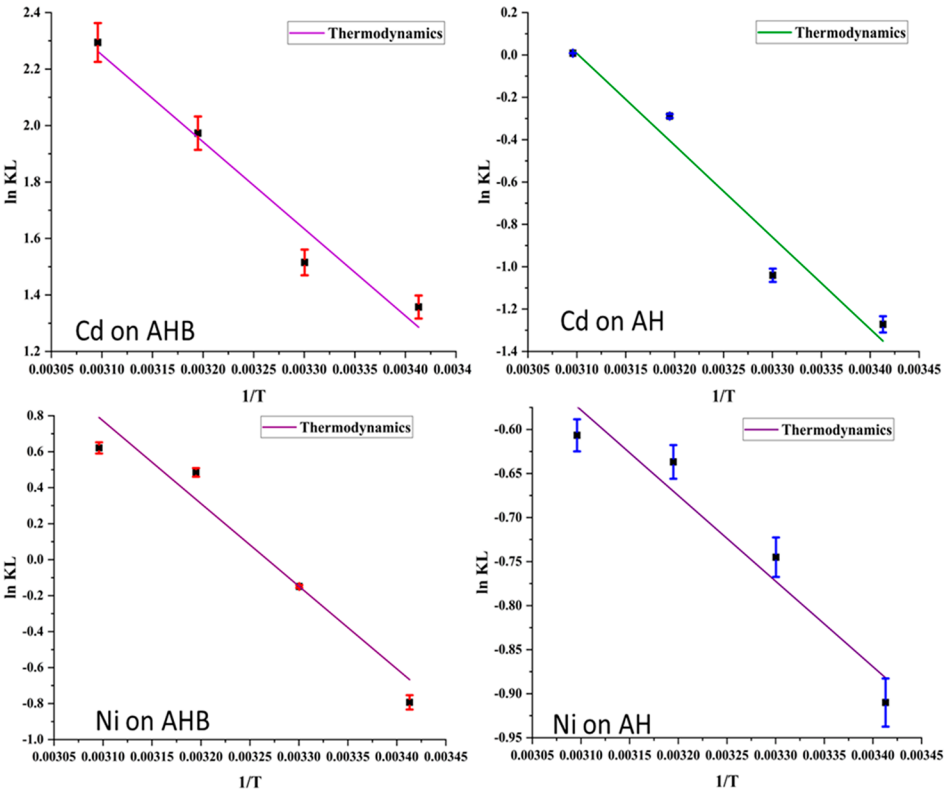

Figure 8. Thermodynamic plot for the adsorption of Cd and Ni on raw *A. hypogaea* (AH) and *A. hypogaea* biochar (AHB).

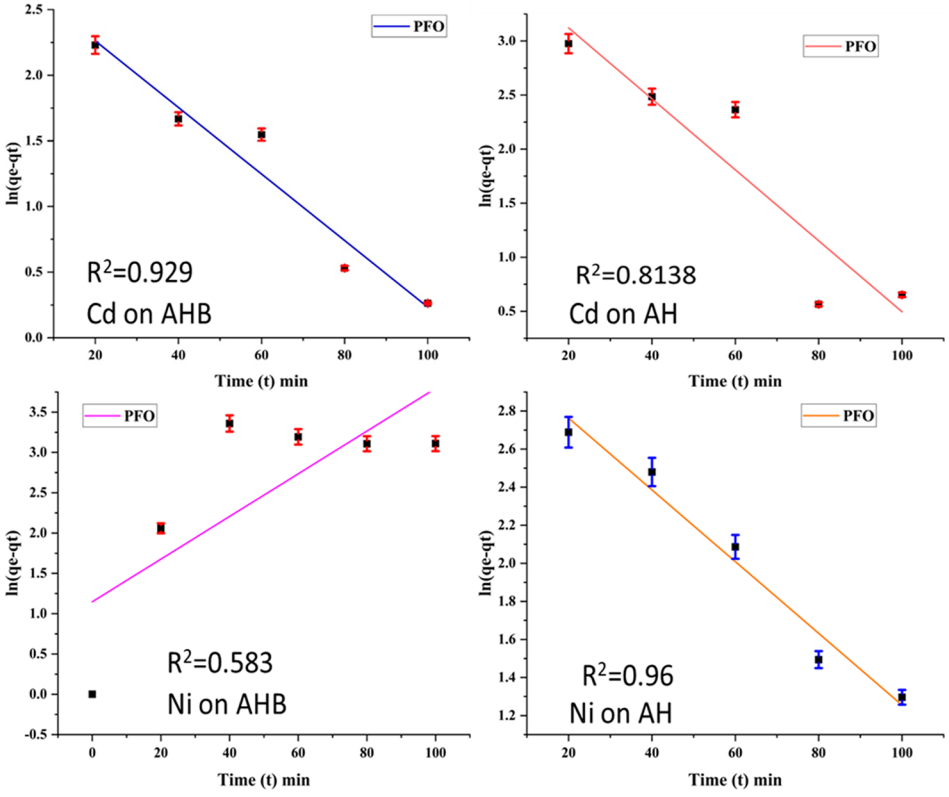

Figure 9. Pseudo-first-order kinetic plot for the adsorption of Cd and Ni on raw *A. hypogaea* (AH) and *A. hypogaea* biochar (AHB).

such as the concentration of sorbate, the time needed for sorption, and the initial concentration of sorbent.[49,50] For evaluation of adsorption parameters, the contact time (10−70 min), initial concentration (20−100 ppm), and amount of adsorbent (0.5−2.5 g) were varied, and the adsorbed amount of metals was studied at equilibrium conditions by an atomic absorption spectrophotometer (AAS 65000 Shimadzu).

https://doi.org/10.1021/acsomega.3c02986
ACS Omega 2023, 8, 40128−40139

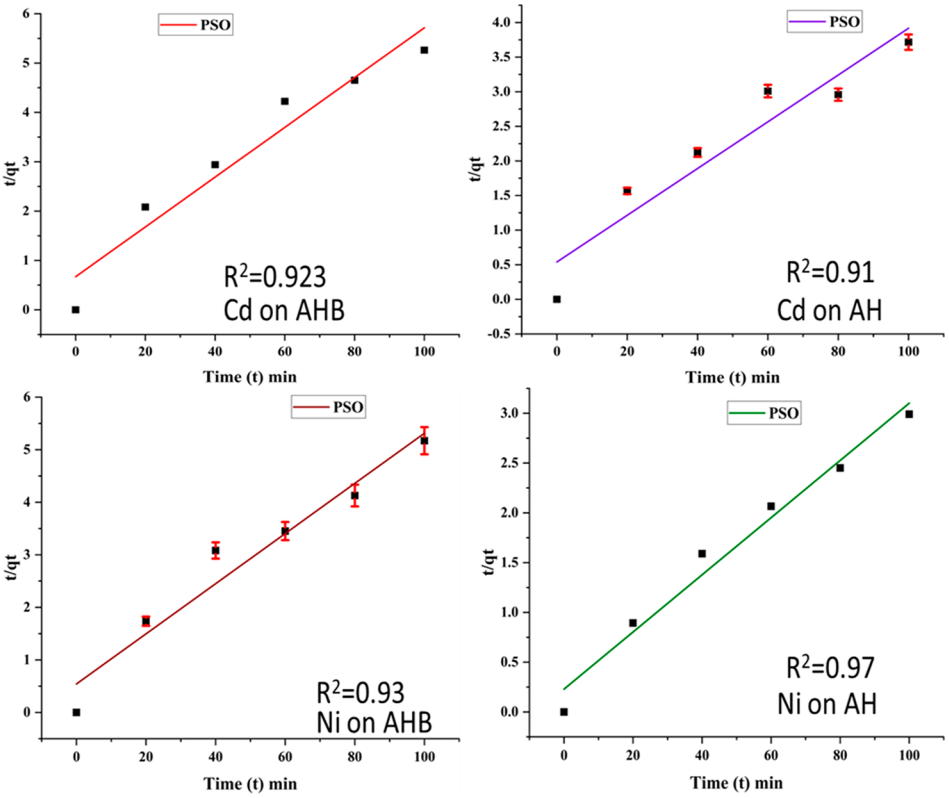

Figure 10. Pseudo-second-order kinetic plot for the adsorption of Cd and Ni on raw *A. hypogaea* (AH) and *A. hypogaea* biochar (AHB).

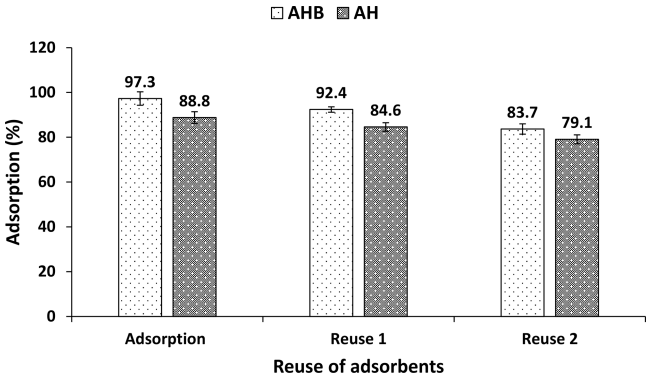

Figure 11. Regeneration and reuse of adsorbents [*A. hypogaea* (AH) and *A. hypogaea* biochar (AHB)] for adsorption purposes.

Equilibrium Isotherms. Adsorption isotherms were designed to study the adsorption pathway as well as the equilibrium relationship of sorbent with sorbate.[51] These isotherms assist in predicting the behavior of the sorbent and different parameters such as thermodynamic and kinetic investigations toward sorption systems.

Isothermal Studies. For thermodynamic studies, the adsorption experiment was carried out at different temperature conditions, and the calculated parameters included enthalpy (ΔH), entropy (ΔS), and Gibbs free energy (ΔG).

Kinetic Parameters. To study the adsorption kinetics, a linear and nonlinear form of pseudo-first and pseudo-second order kinetics was applied to the adsorption data.[52] Adsorption of both metals was obtained at variable time intervals, and kinetic parameters were calculated.

ASSOCIATED CONTENT

Supporting Information

The Supporting Information is available free of charge at https://pubs.acs.org/doi/10.1021/acsomega.3c02986.

Figures S1: Thermogravimetric analysis of *A. hypogaea* (AH) and *A. hypogaea* biochar (AHB); Figure S2: Effect of pH on adsorption of Cd and Ni on *A. hypogaea* biochar (AHB) and *A. hypogaea* (AH); Figure S3: Factors affecting the adsorption of *A. hypogaea* (AH) and *A. hypogaea* biochar (AHB) at pH = 6 (PDF)

AUTHOR INFORMATION

Corresponding Authors

Fozia Batool − *Institute of Chemistry, University of Sargodha, Sargodha 40100, Pakistan;* orcid.org/0000-0001-8023-7558; Email: fozia.batool@uos.edu.pk

Allah Ditta − *Department of Environmental Sciences, Shaheed Benazir Bhutto University Sheringal, Upper Dir 18000, Pakistan; School of Biological Sciences, The University of Western Australia, Perth, WA 6009, Australia;* orcid.org/0000-0003-1745-4757; Email: allah.ditta@sbbu.edu.pk

Authors

Rahman Qadir − *Institute of Chemistry, University of Sargodha, Sargodha 40100, Pakistan;* orcid.org/0000-0002-0112-7594

Fatima Adeeb − *Institute of Chemistry, University of Sargodha, Sargodha 40100, Pakistan*

Samia Kanwal − *Institute of Chemistry, University of Sargodha, Sargodha 40100, Pakistan*

Ehab A. Abdelrahman − *Department of Chemistry, College of Science, Imam Mohammad Ibn Saud Islamic University (IMSIU), Riyadh 11623, Saudi Arabia; Chemistry*

https://doi.org/10.1021/acsomega.3c02986
ACS Omega 2023, 8, 40128−40139

Department, Faculty of Science, Benha University, Benha 13518, Egypt; orcid.org/0000-0003-2493-883X
Sobia Noreen − *Institute of Chemistry, University of Sargodha, Sargodha 40100, Pakistan;* orcid.org/0000-0002-0815-2223
Bedur Faleh A. Albalawi − *Department of Biology, University of Tabuk, Tabuk 47512, Saudi Arabia*
Muhammad Mustaqeem − *Institute of Chemistry, University of Sargodha, Sargodha 40100, Pakistan*
Muhammad Imtiaz − *Soil and Environmental Biotechnology Division, National Institute for Biotechnology and Genetic Engineering (NIBGE), Faisalabad 38000, Pakistan*
Humaira Yasmeen Gondal − *Institute of Chemistry, University of Sargodha, Sargodha 40100, Pakistan;* orcid.org/0000-0001-9532-681X

Complete contact information is available at: https://pubs.acs.org/10.1021/acsomega.3c02986

Author Contributions

Conceptualization: F.B., R.Q., F.A., S.K., E.A.A., S.N., B.F.A.A., M.M., M.I., A.D., and H.Y.G.; Data curation: F.B.; Formal analysis: F.B., R.Q., F.A., S.K., E.A.A., S.N., B.F.A.A., M.M., M.I., A.D., and H.Y.G.; Funding acquisition: B.F.A.A. and A.D.; Investigation: A.A.; Methodology: F.B. and R.Q.; Project administration: F.B. and A.D.; Resources: F.B., R.Q., F.A., S.K., E.A.A., S.N., B.F.A.A., M.M., M.I., A.D., and H.Y.G.; Software: F.B., R.Q., F.A., S.K., E.A.A., S.N., B.F.A.A., M.M., M.I., A.D., and H.Y.G.; Supervision: R.Q.; Validation: F.B., R.Q., F.A., S.K., E.A.A., S.N., B.F.A.A., M.M., M.I., A.D., and H.Y.G.; Visualization: F.B., R.Q., F.A., S.K., E.A.A., S.N., B.F.A.A., M.M., M.I., A.D., and H.Y.G.; Writing−original draft: A.A.; Writing−review and editing: F.B., R.Q., F.A., S.K., E.A.A., S.N., B.F.A.A., M.M., M.I., A.D., and H.Y.G. All authors have read and agreed to the published version of the manuscript.

Notes

The authors declare no competing financial interest.

■ ACKNOWLEDGMENTS

The authors highly acknowledge the Institute of Chemistry, University of Sargodha, Sargodha 40100, Pakistan for the provision of research facilities for the present research work.

■ REFERENCES

(1) Dunlap, R. E.; Catton, W. R. J. Struggling with human exemptionalism: the rise, decline, and revitalization for environmental sociology. *Am. Sociol.* **1994**, *25*, 5−30.
(2) Liang, X.; Su, Y.; Wang, X.; Liang, C.; Tang, C.; Wei, J.; Liu, K.; Ma, J.; Yu, F.; Li, Y. Insights into the heavy metal adsorption and immobilization mechanisms of CaFe-layered double hydroxide corn straw biochar: Synthesis and application in a combined heavy metal-contaminated environment. *Chemosphere* **2023**, *313*, 137467.
(3) Singh, R. L.; Singh, P. K. Global environmental problems. In *Principles and Applications of Environmental Biotechnology for a Sustainable Future*; Springer: Singapore, 2017; pp 13−41.
(4) Thassitou, P. K.; Arvanitoyannis, I. S. Bioremediation: A novel approach to food waste management. *Trends Food Sci. Technol.* **2001**, *12*, 185−196.
(5) Nagajyoti, P.; Lee, K.; Sreekanth, T. Heavy metals, occurrence and toxicity for plants: A review. *Environ. Chem. Lett.* **2010**, *8*, 199−216.
(6) Shi, M.; Xie, Q.; Li, Z. L.; Pan, Y. F.; Yuan, Z.; Lin, L.; Xu, X. R.; Li, H. X. Adsorption of heavy metals on biodegradable and conventional microplastics in the Pearl River Estuary, China. *Environ. Pollut.* **2023**, *322*, 121158.
(7) Pathy, A.; Pokharel, P.; Chen, X.; Balasubramanian, P.; Chang, S. X. Activation methods increase biochar's potential for heavy-metal adsorption and environmental remediation: A global meta-analysis. *Sci. Total Environ.* **2023**, *865*, 161252.
(8) Jitar, O.; Teodosiu, C.; Oros, A.; Plavan, G.; Nicoara, M. Bioaccumulation of heavy metals in marine organisms from the Romanian sector of the Black Sea. *New Biotechnol.* **2015**, *32*, 369−378.
(9) Jaishankar, M.; Tseten, T.; Anbalagan, N.; Mathew, B. B.; Beeregowda, K. N. Toxicity, mechanism and health effects of some heavy metals. *Interdiscip. Toxicol.* **2014**, *7*, 60−72.
(10) Briffa, J.; Sinagra, E.; Blundell, R. Heavy metal pollution in the environment and their toxicological effects on humans. *Heliyon* **2020**, *6* (9), e04691.
(11) Rehman, A. U.; Nazir, S.; Irshad, R.; Tahir, K.; ur Rehman, K.; Islam, R. U.; Wahab, Z. Toxicity of heavy metals in plants and animals and their uptake by magnetic iron oxide nanoparticles. *J. Mol. Liq.* **2021**, *321*, 114455.
(12) Velusamy, S.; Roy, A.; Sundaram, S.; Kumar Mallick, T. A Review on Heavy Metal Ions and Containing Dyes Removal Through Graphene Oxide-Based Adsorption Strategies for Textile Wastewater Treatment. *Chem. Rec.* **2021**, *21*, 1570.
(13) Vardhan, K. H.; Kumar, P. S.; Panda, R. C. A review on heavy metal pollution, toxicity, and remedial measures: Current trends and future perspectives. *J. Mol. Liq.* **2019**, *290*, 111197.
(14) Jiménez, S.; Micó, M. M.; Arnaldos, M.; Medina, F.; Contreras, S. State of the art of produced water treatment. *Chemosphere* **2018**, *192*, 186−208.
(15) Natarajan, S.; Boricha, A. B.; Bajaj, H. C. Recovery of value-added products from cathode and anode material of spent lithium-ion batteries. *Waste Manage.* **2018**, *77*, 455−65.
(16) Igunnu, E. T. *Treatment of produced water by simultaneous removal of heavy metals and dissolved polycyclic aromatic hydrocarbons in a photoelectrochemical cell*; University of Nottingham, 2014.
(17) Shukla, A.; Zhang, Y.-H.; Dubey, P.; Margrave, J. L.; Shukla, S. S. The role of sawdust in the removal of unwanted materials from water. *J. Hazard. Mater.* **2002**, *95*, 137−152.
(18) Katheresan, V.; Kansedo, J.; Lau, S. Y. Efficiency of various recent wastewater dye removal methods: A review. *J. Environ. Chem. Eng.* **2018**, *6*, 4676−4697.
(19) Li, J.; Yu, Y.; Chen, X.; Yu, S.; Cui, M.; Wang, S.; Song, F. Effects of biochar on the phytotoxicity of polyvinyl chloride microplastics. *Plant Physiol. Biochem.* **2023**, *195*, 228−237.
(20) Mamun, S. A.; Saha, S.; Ferdush, J.; Tusher, T. R.; Islam, M. S. Organic amendments for crop production, phosphorus bioavailability, and heavy metal immobilization: a review. *Crop Pasture Sci.* **2022**, *73*, 896.
(21) Alghamdi, A. G.; Alasmary, Z. Efficient Remediation of Cadmium- and Lead-Contaminated Water by Using Fe-Modified Date Palm Waste Biochar-Based Adsorbents. *Int. J. Environ. Res. Public Health* **2023**, *20*, 802.
(22) Yang, X.; Ikehata, K.; Lerner, R.; Hu, Y.; Josyula, K.; Chang, S. X.; Liu, Y. Agricultural Wastes. *Water Environ. Res.* **2010**, *82*, 1396−1425.
(23) Patra, J. M.; Panda, S. S.; Dhal, N. K. Biochar as a low-cost adsorbent for heavy metal removal: A review. *Int. J. Res. Biosci.* **2017**, *6* (1), 1−7.
(24) Shrestha, R.; Ban, S.; Devkota, S.; Sharma, S.; Joshi, R.; Tiwari, A. P.; Kim, H. Y.; Joshi, M. K. Technological trends in heavy metals removal from industrial wastewater: A review. *J. Environ. Chem. Eng.* **2021**, *9*, 105688.
(25) Shao, F.; Xu, J.; Chen, F.; Liu, D.; Zhao, C.; Cheng, X.; Zhang, J. Insights into olation reaction-driven coagulation and adsorption: A pathway for exploiting the surface properties of biochar. *Sci. Total Environ.* **2023**, *854*, 158595.
(26) Foo, K. Y.; Hameed, B. Insights into the modeling of adsorption isotherm systems. *Chem. Eng. J.* **2010**, *156*, 2−10.
(27) Batool, F.; Akbar, J.; Iqbal, S.; Noreen, S.; Bukhari, S. N. A. Study of Isothermal, Kinetic, and Thermodynamic Parameters for Adsorption of Cadmium: An Overview of Linear and Nonlinear Approach and Error Analysis. *Bioinorg. Chem. Appl.* **2018**, *2018*, 1−11.

(28) Awang, N. A.; Wan Salleh, W. N.; Aziz, F.; Yusof, N.; Ismail, A. F. A Review on Preparation, Surface Enhancement and Adsorption Mechanism of Biochar-Supported Nano Zero-Valent Iron Adsorbent for Hazardous Heavy Metals. *J. Chem. Technol. Biotechnol.* **2023**, *98*, 22−44.
(29) Al-Ghouti, M. A.; Da'ana, D. A. Guidelines for the Use and Interpretation of Adsorption Isotherm Models: A Review. *J. Hazard. Mater.* **2020**, *393*, 122383.
(30) Wu, M.; Liu, B.; Li, J.; Su, X.; Liu, W.; Li, X. Influence of pyrolysis temperature on sludge biochar: the ecological risk assessment of heavy metals and the adsorption of Cd (II). *Environ. Sci. Pollut. Res.* **2023**, *30* (5), 12608−12617.
(31) Mrad, R.; Chehab, G. Mechanical and Microstructure Properties of Biochar-Based Mortar: An Internal Curing Agent for PCC. *Sustainability* **2019**, *11*, 2491.
(32) Akpomie, K. G.; Dawodu, F. A. Potential of low-cost bentonite for heavy metal abstraction from the binary component system. *Beni-Suef Univ. J. Basic Appl. Sci.* **2015**, *4*, 1−13.
(33) Limousin, G.; Gaudet, J.-P.; Charlet, L.; Szenknect, S.; Barthès, V.; Krimissa, M. Sorption isotherms: A review on physical bases, modeling, and measurement. *Appl. Geochem.* **2007**, *22*, 249−275.
(34) Zhou, Y.; Zou, Z.; Wang, M.; Wang, Y.; Li, J.; Qiu, L.; Cheng, Y.; Dai, Z. Biochar and nano-ferric oxide synergistically alleviate cadmium toxicity of muskmelon. *Environ. Sci. Pollut. Res.* **2023**, *30*, 57945−57959.
(35) Ye, H.; Yu, K.; Li, B.; Guo, J. Study on adsorption properties and mechanism of sodium hydroxide-modified ball-milled biochar to dislodge lead(II) and MB from water. *Biomass Conv. Bioref.* **2023**, 1−15.
(36) Basu, S.; Shivhare, U. S.; Mujumdar, A. S. Models for sorption isotherms for foods: A review. *Dry. Technol.* **2006**, *24*, 917−930.
(37) Khaled, A.; Nemr, A. E.; El-Sikaily, A.; Abdelwahab, O. Removal of Direct N Blue-106 from artificial textile dye effluent using activated carbon from orange peel: Adsorption isotherm and kinetic studies. *J. Hazard. Mater.* **2009**, *165*, 100−110.
(38) Hu, X.; Chen, C.; Zhang, D.; Xue, Y. Kinetics, isotherm and chemical speciation analysis of Hg(II) adsorption over oxygen-containing MXene adsorbent. *Chemosphere* **2021**, *278*, 130206.
(39) Bayuo, J.; Rwiza, M.; Mtei, K. Response surface optimization and modeling in heavy metal removal from wastewater - A critical review. *Environ. Monit. Assess.* **2022**, *194* (5), 351.
(40) Tong, X.; Song, Q.; Wang, L.; Hong, Z.; Dong, Y.; Jiang, J. Effects of biochars derived from four crop straws on a Cd-polluted cinnamon soil. *Environ. Sci. Pollut. Res.* **2023**, *30* (9), 24764−24770.
(41) Tungala, L. S.; Mekala, S.; Pala, S. L.; Biftu, W. K.; Ravindhranath, K. Stem powder and its active carbon of Arachis hypogaea plant for lead (II) removal: application to treat battery-based industrial effluents. *Int. J. Phytoremediation* **2023**, *25* (5), 598−608.
(42) Lin, H.; Yang, D.; Zhang, C.; Liu, W.; Zhang, L.; Dong, Y. Selective removal behavior of lead and cadmium from calcium-rich solution by MgO loaded soybean straw biochars and mechanism analysis. *Chemosphere* **2023**, *319*, 138010.
(43) Murtaza, G.; Ahmed, Z.; Dai, D.-Q.; Iqbal, R.; Bawazeer, S.; Usman, M.; Rizwan, M.; Iqbal, J.; Akram, M. I.; Althubiani, A. S.; Tariq, A.; Ali, I. A review of mechanism and adsorption capacities of biochar-based engineered composites for removing aquatic pollutants from contaminated water. *Front. Environ. Sci.* **2022**, *10*, 2155.
(44) Pathirana, C.; Ziyath, A. M.; Egodawatta, P.; Bandara, N. J.; Jinadasa, K. B. S. N.; Bandala, E. R.; Wijesiri, B.; Goonetilleke, A. Biosorption of heavy metals: Transferability between batch and column studies. *Chemosphere* **2022**, *294*, 133659.
(45) Argun, M. E.; Dursun, S.; Ozdemir, C.; Karatas, M. Heavy metal adsorption by modified oak sawdust: Thermodynamics and kinetics. *J. Hazard. Mater.* **2007**, *141*, 77−85.
(46) Manikandan, S. K.; Pallavi, P.; Shetty, K.; Bhattacharjee, D.; Giannakoudakis, D. A.; Katsoyiannis, I. A.; Nair, V. Effective Usage of Biochar and Microorganisms for the Removal of Heavy Metal Ions and Pesticides. *Molecules* **2023**, *28* (2), 719.
(47) Li, J.; Dong, X.; Liu, X.; Xu, X.; Duan, W.; Park, J.; Gao, L.; Lu, Y. Comparative Study on the Adsorption Characteristics of Heavy Metal Ions by Activated Carbon and Selected Natural Adsorbents. *Sustainability* **2022**, *14* (23), 15579.
(48) Li, Y.; Yin, H.; Cai, Y.; Luo, H.; Yan, C.; Dang, Z. Regulating the exposed crystal facets of α-Fe_2O_3 to promote Fe_2O_3-modified biochar performance in heavy metals adsorption. *Chemosphere* **2023**, *311*, 136976.
(49) Ke, Y.; Zhang, F.; Zhang, Z.; Hough, R.; Fu, Q.; Li, Y. F.; Cui, S. Effect of combined aging treatment on biochar adsorption and speciation distribution for Cd (II). *Sci. Total Environ.* **2023**, *867*, 161593.
(50) Kochar, C.; Taneja, L.; Yadav, P. K.; Tripathy, S. S. RSM-CCD approach for optimization study on effective remediation of lead and cadmium from water using surface-modified water caltrop peel biochar. *Biomass Conv. Bioref.* **2023**, DOI: 10.1007/s13399-023-04013-2.
(51) Wang, Q.; Wen, J.; Yang, L.; Cui, H.; Zeng, T.; Huang, J. Exploration of the role of different iron species in the remediation of As and Cd co-contamination by sewage sludge biochar. *Environ. Sci. Pollut. Res.* **2023**, *30*, 39154−39168.
(52) Zhou, P. F.; Adeel, M.; Guo, M. L.; Ge, L.; Shakoor, N.; Li, M. S.; Li, Y. B.; Wang, G. Y.; Rui, Y. K. Characterisation of biochar produced from two types of chestnut shells for use in remediation of cadmium- and lead-contaminated soil. *Crop Pasture Sci.* **2022**, *74*, 147.

https://doi.org/10.1021/acsomega.3c02986
ACS Omega 2023, 8, 40128−40139